



## Research Article

# Investigation of friction behavior of $TiO_2: Al_2O_3$ composite coating formed on AA2024 alloy by micro-arc oxidation

Emine BOYNUEĞRİ KAPLAN<sup>1,\*</sup>, Ebru Emine ŞÜKÜROĞLU<sup>1</sup>

<sup>1</sup>Department of Mechanical Engineering, Gumushane University, Gumushane, Türkiye

## ARTICLE INFO

### Article history

Received: 30 December 2021

Revised: 11 March 2022

Accepted: 22 April 2022

### Keywords:

AA2024 Alloy;  $Al_2O_3$ ;  $TiO_2$ ;

$Al_2O_3$ ; Composite Coating;

Micro Arc Oxidation (MAO)

## ABSTRACT

In this study, an alumina ( $Al_2O_3$ ) ceramic coating and a composite coating containing titanium dioxide ( $TiO_2$ ) particles were prepared on surfaces of AA2024 substrates by micro-arc oxidation (MAO) treatment. The effects of micro-sized ( $\approx 20-30 \mu m$ )  $TiO_2$  particles incorporated into electrolyte on the microstructure, phase and chemical composition, thickness, and friction behavior of the coating were investigated. The surface morphologies of the coatings were analyzed by scanning electron microscopy (SEM). The phase and chemical compositions of the coatings were evaluated by means of X-ray diffraction (XRD) and energy-dispersive X-ray spectrometry (EDS), respectively. The friction coefficient of the coatings was investigated using a pin-on-disc tribometer under condition of dry slip sliding. Moreover, the wear tracks were analyzed by SEM. Addition of  $TiO_2$  particles into the electrolyte resulted in the reduction in number of pores and formation of smaller and more uniform pores in comparison with the  $Al_2O_3$  ceramic coating. XRD analyses demonstrated that the  $TiO_2:Al_2O_3$  composite coating was composed of anatase- $TiO_2$  and rutile- $TiO_2$ , as well as pure aluminum,  $\alpha-Al_2O_3$  and  $\gamma-Al_2O_3$  which are the primary phases. The friction tests showed a significant reduction in the friction coefficient of the composite coated samples which contains titanium oxide ( $TiO_2$ ) particles in comparison with  $Al_2O_3$  coated and uncoated samples.

**Cite this article as:** Boynueğri Kaplan E, Şüküroğlu EE. Investigation of friction behavior of  $TiO_2: Al_2O_3$  composite coating formed on AA2024 alloy by micro-arc oxidation. Sigma J Eng Nat Sci 2024;42(1):63–69.

## INTRODUCTION

The usage of aluminum (Al) alloys is increasing rapidly every year in industrial and engineering applications such as automotive, rail transport, shipbuilding, aviation, aerospace and construction sectors. [1-9]. The main causes for the increasing popularity of Al alloys are their versatile properties such as high specific strength, low weight,

relatively low cost, good corrosion resistance, formability and recyclability. [6, 10]. However, their poor surface characteristic, especially low surface hardness, high friction coefficient and poor wear resistance have greatly limited their range of tribological applications. [2, 11]. Thus, surface treatment technologies have been playing a key role in enhancing their usability of aluminum alloys. [12-17].

### \*Corresponding author.

\*E-mail address: boynuegriemine@gmail.com

This paper was recommended for publication in revised form by Regional Editor Fatih Akyol



Micro arc oxidation (MAO) is a simple and effective surface treatment for forming ceramic-like coating films on metals. [12, 16]. This method is a rapid development new technology in recent years. To date, the materials most coated with MAO treatment are aluminum [18], titanium [19], magnesium [20], zinc [21] and their alloys. The coating films fabricated by MAO can have a series advantage such as high corrosion resistance, high wear resistance, uniform thickness and ideal adhesive strength to the substrate. [12, 16-18]. The composition of substrate materials and electrolyte, electrical parameters, processing temperature, oxidation time, type and size of additive have a large impact on the properties of MAO coatings. [17]. Thus, the ideal properties can be achieved by controlling the process parameters.

The substrate material plays a critical role in the components and properties of MAO coatings. In the other words, the dominant compositions of the MAO coatings depend on the substrate material. For example, the main content of the coatings formed on aluminum, magnesium, titanium and their alloys are  $\text{Al}_2\text{O}_3$ ,  $\text{MgO}$  and  $\text{TiO}_2$ , respectively. Furthermore, the additions of different particles in the electrolyte can affect the MAO treatment, and significantly change further the microstructure and the property of the coatings. [12, 22]. Recent studies have shown that the composite coatings obtained by adding of  $\text{TiO}_2$  into the electrolyte have given better wear performance. [23-25]. However, there has been limited study on the tribological properties of  $\text{TiO}_2$ -doped  $\text{Al}_2\text{O}_3$  composite coating formed on AA2024 alloy. [24].

Since the differences in substrate material result in different growth rates, structures, phase composition and element distribution of the MAO coatings,  $\text{TiO}_2$ : $\text{Al}_2\text{O}_3$  composite coating was formed on AA2024 aluminum alloy by MAO treatment with present study. The main motivation for this study is to add a new resource to the limited publication. The characterization of the coating surface was analyzed scanning electron microscopy (SEM), X-ray diffraction (XRD) and energy-dispersive X-ray spectrometry (EDS), respectively. The friction behavior of the coating was determined using a pin-on-disc tribometer at the dry sliding conditions. The effect of the  $\text{TiO}_2$  particles incorporated into electrolyte on the surface morphology, coating thickness and coefficient of friction was investigated.

## MATERIALS AND METHODS

AA2024 is one of the most widely used groups of aluminium alloys and have been extensively used for

automotive and aerospace industries due to high strength and excellent machinability. [9, 27]. AA2024 alloy was used to as the substrate material. The chemical composition of AA2024 is shown in Table 1.

The samples with dimension 20x20x2 mm were successively polished with silicon carbide (SiC) papers of grit numbers of 400, 800 and 1200. Then, polished samples were rinsed with ethanol and dried prior to MAO process. The surface roughness values of the polished samples were measured approximately  $R_a \approx 0.10\text{-}0.13 \mu\text{m}$  by MarSurf PS1 tester. The MAO treatment of AA2024 substrates were carried out by the MAO system which was designed and manufactured by Plasma Technology Ltd. Two different electrolytes were prepared for the MAO process. The base electrolyte consisted of KOH (1 g/L),  $\text{Na}_2\text{SiO}_3$  (2 g/L) and  $\text{Al}_2\text{O}_3$  (3 g/L) and distilled water. The second electrolyte contained  $\text{TiO}_2$  (3 g/L) particles, approximately  $\approx 20\text{-}30 \mu\text{m}$  in size, incorporated into the base electrolyte under similar conditions. An AC power supply was used in bipolar mode. The MAO process was performed with frequency of 700 Hz and a voltage of 550 V at 10 minutes operating time. The AA2024 samples and stainless-steel bath walls were set as the anode and cathode, respectively. The temperature of electrolytes was kept below 30 °C using a cooling system. After the MAO treatment, the samples were cleaned with ethanol and dried.

The surface morphologies and thickness of the coatings were analyzed by scanning electron microscopy and chemical composition of the coatings by SEM-EDS (Model: QUANTA 250 FEG). The coated samples were immersed in a liquid nitrogen bath and broke brittle to establish the coating thickness. The phase was analyzed by means of X-ray diffraction (Model: Malvern Panalytical Empyrean). XRD analysis was conducted with a scanning rate of  $2^\circ/\text{min}$  from  $20^\circ$  to  $90^\circ$  ( $2\theta$ ) at a wavelength of  $\lambda = 1.5404 \text{ \AA}$ . The phases were defined by comparing the reflections obtained after the analysis with the peak lists of the JCPDS (Joint Committee on Powder Diffraction Standards). After MAO treatments, the friction behavior of the coatings was investigated under condition of dry slip sliding. The friction coefficient of uncoated and coated samples against the  $\text{Al}_2\text{O}_3$  ball were determined under 2N load. Then, the wear tracks were analyzed by SEM.

## RESULTS AND DISCUSSION

The surface morphologies of the  $\text{Al}_2\text{O}_3$  coating and  $\text{TiO}_2$ : $\text{Al}_2\text{O}_3$  composite coating are shown in Figure 1. In general, the MAO is carried out at the voltages higher than

**Table 1.** The Chemical Composition of AA2024 Substrate

Element	Cu	Mg	Mn	Fe	Si	Zn	Cr	Al
(wt.%)	4.4	1.5	0.6	0.5	0.5	0.25	0.1	Balance

the breakdown voltage of the passive oxide film preformed on the surface and it is characterized by electrical sparks appeared on the anode surface. [12, 16]. During the process, micro-pores develop in the layer which grows by the continuous discharge process. These micro-pores allow continuing current flow and thus film growth. [16, 17]. As seen in Figure 1 (a, b), it is observed that the micro-pores have different diameters and random location on the surfaces. During the process, the irregular melting of Al has resulted in formation of some porosities, empty inclusions and volcanic formations. Moreover, there is few micro-cracks on the surface of MAO coating (Figure 1(a)). These pores and cracks formations are caused by molten oxide and gas bubbles thrown out of micro-arc discharge channels as a result of the nature of the MAO process. The cracks resulted from the thermal stress due to the rapid solidification of the molten oxide. [16-18, 28]. When Figure 1(b) is examined detail, it can be seen that less porous surface of composite coating which doped with  $\text{TiO}_2$  particles. Moreover, pores are more

uniform in both size and shape. This is due to the strong adhesion of the additive to the surface and the filling of the discharge channels by  $\text{TiO}_2$  particles. [24, 29]. In other words, the addition of  $\text{TiO}_2$  particles relatively resulted in a decrease of pore diameter. Moreover, the addition of  $\text{TiO}_2$  particles resulted in an increase of the coating compactness.

Figure 2 (a), (b) shows the cross-sectional images of  $\text{Al}_2\text{O}_3$  coating and composite coating contained  $\text{TiO}_2$  particles, respectively. When the coating thicknesses grown on the surface are examined, the thickness of layer was obtained as  $\approx 24 \mu\text{m}$  in the  $\text{Al}_2\text{O}_3$  coated sample, while the thickness was obtained as approximately  $\approx 32 \mu\text{m}$  in the  $\text{TiO}_2$  doped  $\text{Al}_2\text{O}_3$  coated sample. This growth is thought to be due to the  $\text{TiO}_2$  particles were placed among the micropores. This trend is the expected situation in MAO processes. It can be seen that these pores in Figure 1 (b) are fuller and uniform. This is the explanation that the pores are filled during the coating. In fact,  $\text{TiO}_2$  particles increased the conductivity of the MAO electrolyte. The previous studies based

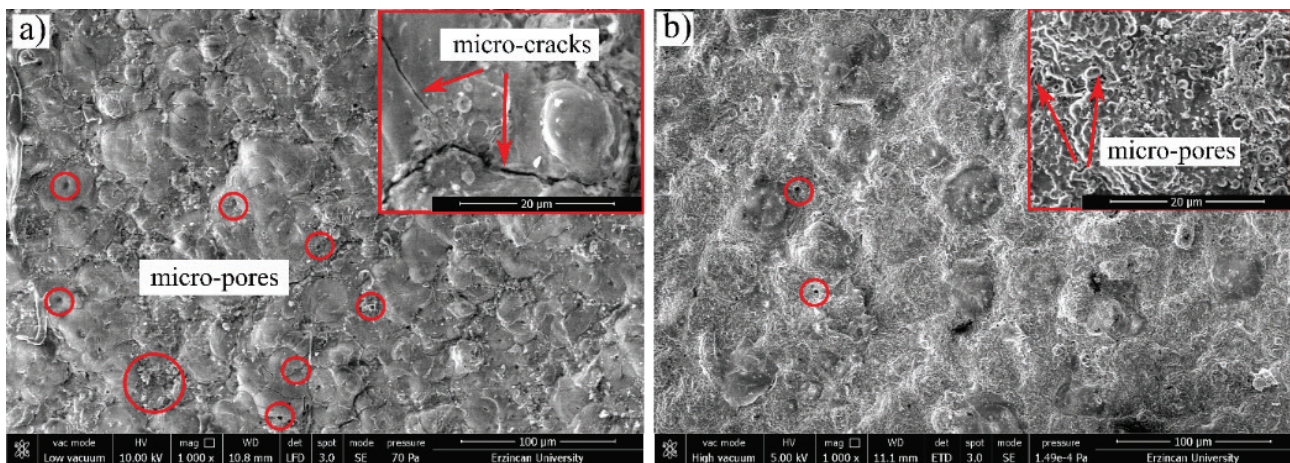


Figure 1. SEM images of (a)  $\text{Al}_2\text{O}_3$  coating, (b)  $\text{TiO}_2:\text{Al}_2\text{O}_3$  composite coating.

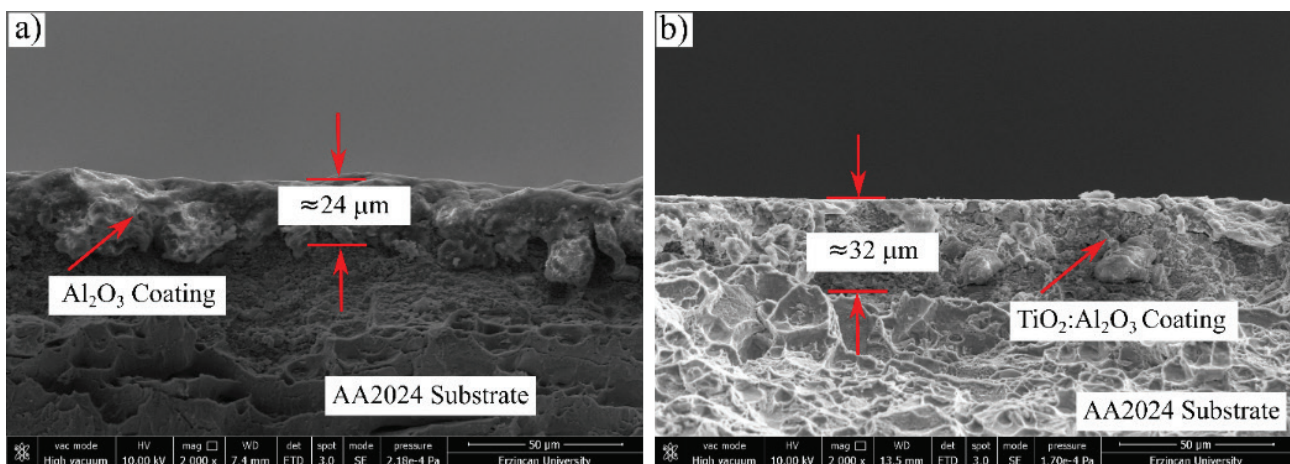
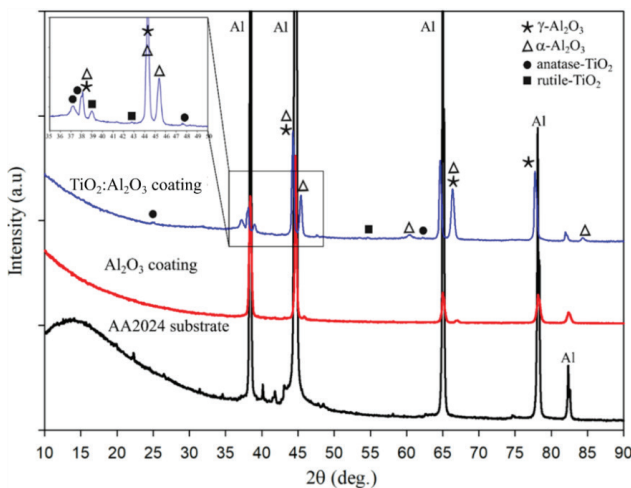


Figure 2. Cross-sectional microstructure for (a)  $\text{Al}_2\text{O}_3$  coating, (b)  $\text{TiO}_2:\text{Al}_2\text{O}_3$  composite coating.

on production of composite coatings containing micro or nano  $\text{TiO}_2$  particles have shown an increase in coating layer thickness. [24, 29].

XRD graphs of the AA2024 sample and coated samples are shown in Figure 3. It is found that coated samples are mainly composed of Al,  $\alpha\text{-Al}_2\text{O}_3$  and  $\gamma\text{-Al}_2\text{O}_3$ . In addition, Al peak with intensity and much stronger was observed in the uncoated sample. After both MAO treatment, it was clearly seen that the intensity of Al peak has decreased. It can be said that the high-density peaks of Al come from the AA2024 substrate. The  $\gamma\text{-Al}_2\text{O}_3$  characteristic peaks were observed at  $2\theta \approx 38^\circ$ ,  $2\theta \approx 44^\circ$ ,  $2\theta \approx 66^\circ$  and  $2\theta \approx 78^\circ$  corresponding to planes (311), (400), (440) and (533), respectively. The  $\alpha\text{-Al}_2\text{O}_3$  characteristic peaks were also detected at  $2\theta \approx 46^\circ$ ,  $2\theta \approx 66^\circ$  and  $2\theta \approx 84^\circ$  corresponding to planes (012), (202) and (223), respectively.

These peaks correspond to both  $\gamma\text{-Al}_2\text{O}_3$  and  $\alpha\text{-Al}_2\text{O}_3$  as mentioned in previous literature. [30–32]. High pressure



**Figure 3.** XRD graphs of AA2024 sample,  $\text{Al}_2\text{O}_3$  coating and  $\text{TiO}_2:\text{Al}_2\text{O}_3$  composite coating.

and temperature helped to form the  $\alpha\text{-Al}_2\text{O}_3$  and  $\gamma\text{-Al}_2\text{O}_3$  phases easily. The XRD graphs in Figure 3 show clear differences in phases between the  $\text{Al}_2\text{O}_3$  coating and the  $\text{TiO}_2$ -doped  $\text{Al}_2\text{O}_3$  composite coating. The anatase- $\text{TiO}_2$  and rutile- $\text{TiO}_2$  phases on surface of the  $\text{TiO}_2:\text{Al}_2\text{O}_3$  composite coating were identified. This finding indicates that  $\text{TiO}_2:\text{Al}_2\text{O}_3$  composite coating had been successfully grown on AA2024 alloy using MAO treatment. Similar to the literature, the intensity of anatase- $\text{TiO}_2$  and rutile- $\text{TiO}_2$  phases was determined at  $2\theta \approx 25.2^\circ$ ,  $2\theta \approx 36.9^\circ$ ,  $2\theta \approx 37.7^\circ$ ,  $2\theta \approx 38.5^\circ$ ,  $2\theta \approx 42.3^\circ$ ,  $2\theta \approx 48^\circ$ ,  $2\theta \approx 55.1^\circ$  and  $2\theta \approx 62.60^\circ$  corresponding to planes (101), (103), (004), (200), (111), (200), (211) and (204), respectively. [33, 35].

The energy-dispersive X-ray spectrometry (EDS) analysis of the surface of  $\text{TiO}_2:\text{Al}_2\text{O}_3$  composite coating is shown in Figure 4. The results showed that the coating consists mainly of aluminum (Al), oxygen (O), titanium (Ti) and silicon (Si) with an atomic concentration of 41.85%, 52.14%, 3.61%, and 2.41%, respectively. The concentration of the titanium in the coating is greatly lower than aluminum and oxygen. From the literature, it is well known that silicon comes from the composition of electrolyte used in the growth of the composite coating. [29]. In fact, Figure 1 (b) shows that the  $\text{TiO}_2$  particles were dispersed all over the surface of coating. Also from Figure 2, it is seen that the phases of  $\text{TiO}_2$  particles were detected on the surface of coating. Lastly, the EDS results indicated that  $\text{TiO}_2:\text{Al}_2\text{O}_3$  composite coating has been successfully grown on AA2024 alloy using MAO treatment.

The friction coefficient (COF) of the uncoated AA2024 alloy and  $\text{Al}_2\text{O}_3$  coated and  $\text{TiO}_2:\text{Al}_2\text{O}_3$  composite coated samples were evaluated by pin-on disk tribometer using  $\text{Al}_2\text{O}_3$  ball as counterpart material. Firstly, the COF graphs were determined. Then the wear tracks were analyzed by SEM in order to identify the wear mechanism of coatings. The experiments were performed at total sliding distance of 60 m under 2N load for all samples. Figure 5 shows the changes in the COF as a function of sliding distance.

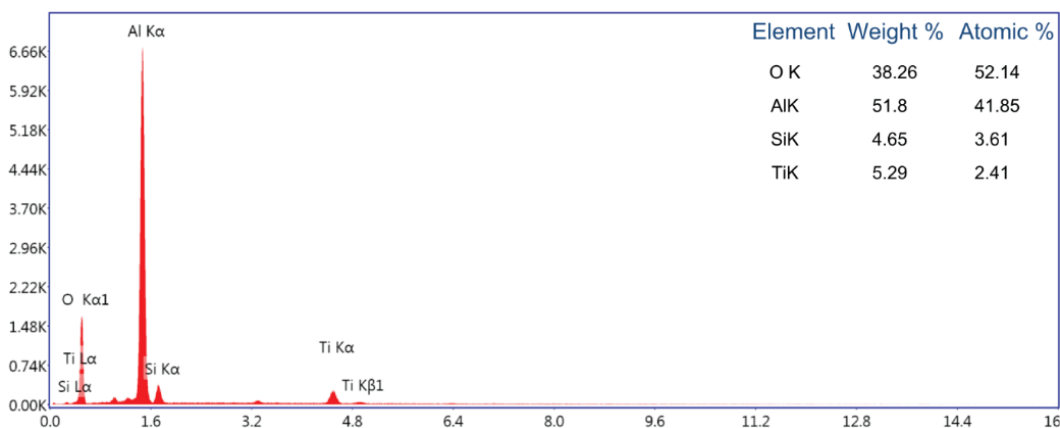


**Figure 4.** EDS analysis of the  $\text{TiO}_2:\text{Al}_2\text{O}_3$  composite coating.

AA2024 substrate showed that the average COF value of 0.57-0.58 during the steady stage. The friction coefficient increased rapidly in the initial stages and then gradually decreased. After 10m, the friction coefficient became stable.  $\text{Al}_2\text{O}_3$  coating and  $\text{TiO}_2:\text{Al}_2\text{O}_3$  composite coating exhibited lower initial COF value than the uncoated AA2024 sample. During the test, it was observed that there was severe plastic deformation on the substrate.

The friction coefficient of both coated samples are much lower than that of the substrate. However, the samples covered by the progress of the test period have been found to have significant fluctuations in the coefficients of friction. This can be explained by the rapid occurrence of three body wear, especially in coatings produced with the addition of  $\text{TiO}_2$  particles. [23, 24]. Adding  $\text{TiO}_2$  particle affected the friction coefficient values. The lowest friction coefficient value was obtained with novel  $\text{TiO}_2$  doped  $\text{Al}_2\text{O}_3$  composite coated sample. The friction coefficient of the  $\text{TiO}_2:\text{Al}_2\text{O}_3$  composite coating was obviously decreased because of the strong adhesion of the  $\text{TiO}_2$  particles to the surface and the filling of the discharge channels by these particles. [23-26, 29, 35]. Previous studies has shown that the anatase- $\text{TiO}_2$ , rutile- $\text{TiO}_2$  particles lead to achieve a compact and uniform morphology of coating surface that can reduce the friction coefficient of the substrate. [26, 35, 36]. Some  $\text{TiO}_2$  particles

that are not tightly connected act as the third body rigid particles that are harmful to the coating itself. However, it is known that the rutile phase of  $\text{TiO}_2$  is a phase that is more resistant to wear and can contribute in addition to the lower wear performance. [26].

Figure 5 also displays the SEM images of the wear tracks morphologies of the AA2024 substrate,  $\text{Al}_2\text{O}_3$  coating and  $\text{TiO}_2:\text{Al}_2\text{O}_3$  composite coating. As shown in Figure 5, the average width of the wear marks decreases as a function of the coating. This can be explained by the sample being worn and the applied coating creating a barrier against wear on the surface. Compared to the AA2024 substrates, both coatings have been observed to be shallow and narrow. AA2024 substrate showed signs of plastic deformation in combination with adhesive and abrasive wear. Some micro cracks were also observed and most of loosen wear debris were found in the wear track as shown in Figure 5 (a). The wear mechanism of the  $\text{Al}_2\text{O}_3$  coating consisted mainly of micro cracks and the removal of the coating as flakes accompanied by the formation of the protective transfer layer as shown in Figure 5 (b). It is thought that the roughness on the surface of the  $\text{Al}_2\text{O}_3$  coating ensures the adherence of the tribolayer by mechanical interlocking. [18]. Meanwhile, AA2024 substrate is directly oxidized to become  $\alpha\text{-Al}_2\text{O}_3$  and  $\gamma\text{-Al}_2\text{O}_3$  phases due to a high temperature in the microarc zone. So, there is an ideal adhesion between the  $\text{Al}_2\text{O}_3$  ceramic coating and AA2024 substrate. [37, 38]. The addition of  $\text{TiO}_2$  particles resulted in an increase of the coating compactness and affect wear mechanism of the coating. The addition of  $\text{TiO}_2$  particles into electrolyte the abrasive wear and detachment of the coating was effectively reduced as shown in Figure 5 (c). This is believed to be due to an increase in the thickness of the coating with the addition of  $\text{TiO}_2$  particles, as well as the capacity to carry loads.

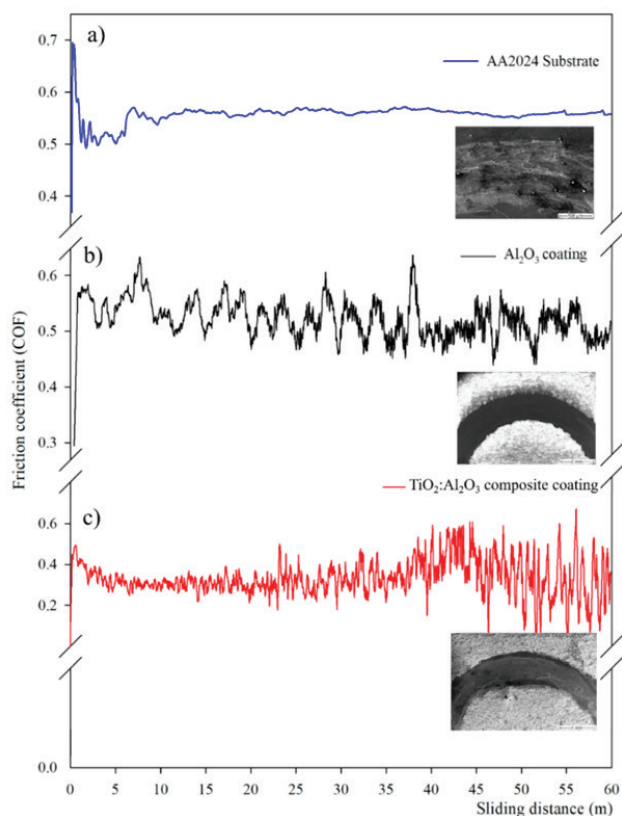


**Figure 5.** Coefficient of friction graphs of (a) AA2024 sample, (b)  $\text{Al}_2\text{O}_3$  coating, (c)  $\text{TiO}_2:\text{Al}_2\text{O}_3$  composite coating.

## CONCLUSION

In this study,  $\text{Al}_2\text{O}_3$  coating and  $\text{TiO}_2:\text{Al}_2\text{O}_3$  composite coating layer were formed on AA2024 alloy by micro arc oxidation (MAO) method. The effects of  $\text{TiO}_2$  particles incorporated into electrolyte on the microstructure, phase and chemical composition, thickness, and friction behavior of the coating were investigated. The results from this study obtained are summarized below.

- i. MAO coating was successfully applied to AA2024 alloy for the  $\text{TiO}_2$ -doped  $\text{Al}_2\text{O}_3$  ceramic coating.
- ii. It was concluded that the addition of  $\text{TiO}_2$  particles into the electrolyte resulted in the reduction in number of pores and formation of smaller and more uniform pores in comparison with the  $\text{Al}_2\text{O}_3$  coating.
- iii. With X-ray Diffraction (XRD) analyses, it was found that both coated samples are mainly composed of Al,  $\alpha\text{-Al}_2\text{O}_3$  and  $\gamma\text{-Al}_2\text{O}_3$ . Moreover, presence of rutile and anatase phases characterizing  $\text{TiO}_2$  was detected on the surface of composite coating. The micro pores and

micro cracks on the composite coating were filled with TiO<sub>2</sub> particles in the MAO treatment.

- iv. The EDS results showed that the composite coating consists mainly of aluminum (Al), oxygen (O), titanium (Ti) and silicon (Si) with an atomic concentration of 41.85%, 52.14%, 3.61%, and 2.41%, respectively.
- v. The average coefficient of the Al<sub>2</sub>O<sub>3</sub> coating and TiO<sub>2</sub>:Al<sub>2</sub>O<sub>3</sub> composite coating are 0.5 and 0.36, respectively. Adding TiO<sub>2</sub> particle affected the friction coefficient values. The lowest friction coefficient value was obtained with novel TiO<sub>2</sub> doped Al<sub>2</sub>O<sub>3</sub> composite coated sample.
- vi. Compared to AA2024 alloy, an improvement of approximately 60% was observed in the COF value with the composite coating containing titanium dioxide (TiO<sub>2</sub>) particles formed on surface of AA2024.
- vii. The addition of TiO<sub>2</sub> particles resulted in an increase of the coating compactness and affect wear mechanism of the coating.
- viii. The addition of TiO<sub>2</sub> particles resulted in an increase of the coating thickness, as well as the capacity to carry loads.
- ix. The addition of TiO<sub>2</sub> particles into electrolyte the abrasive wear and detachment of the coating was effectively reduced.

## AUTHORSHIP CONTRIBUTIONS

Authors equally contributed to this work.

## DATA AVAILABILITY STATEMENT

The authors confirm that the data that supports the findings of this study are available within the article. Raw data that support the finding of this study are available from the corresponding author, upon reasonable request.

## CONFLICT OF INTEREST

The author declared no potential conflicts of interest with respect to the research, authorship, and/or publication of this article.

## ETHICS

There are no ethical issues with the publication of this manuscript.

## REFERENCES

- [1] Miller WS, Zhuang L, Bottema J, Wittebrood AJ, De Smet P, Haszler A, Vieregge A. Recent development in aluminium alloys for the automotive industry. *Mater Sci Eng A* 2000;280:37–49. [\[CrossRef\]](#)
- [2] Dursun T, Soutis C. Recent developments in advanced aircraft aluminium alloys. *Mater Des* 2014;56:862–871. [\[CrossRef\]](#)
- [3] Hirsch J. Recent development in aluminium for automotive applications. *Trans Nonferrous Metals Soc China* 2014;24:1995–2002. [\[CrossRef\]](#)
- [4] Çam G, İpekoğlu G. Recent developments in joining of aluminum alloys. *Int J Adv Manuf Technol* 2017;91:1851–1866. [\[CrossRef\]](#)
- [5] Bolat Ç, Akgün IC, Goksenli A. On the way real applications: aluminum matrix syntactic foams. *Eur Mech Sci* 2020;4:131–141. [\[CrossRef\]](#)
- [6] Banhart J. Aluminum foams: on the road to real applications. *MRS Bull* 2003;28:290–295. [\[CrossRef\]](#)
- [7] Öcalır Ş, Eşme U, Boğa C, Külekci MK. Investigation of mechanical and metallographic of two different aluminum alloys joined with friction stir welding method using different welding parameters. *Sigma J Eng Nat Sci* 2020;38:1333–1349.
- [8] Akkuş H, Düzcükoğlu H, Şahin ÖS. Experimental design for bending strength aluminum honeycomb structure. *Sigma J Eng Nat Sci* 2016;34:555–561.
- [9] Kasman Ş, Ozan S. An experimental approach for friction stir welding: A case study for AA-2024-T351. *Sigma J Eng Nat Sci* 2020;38:1999–2011.
- [10] Mondolfo LF. *Aluminum alloys: Structure and properties*. London: Butterworth; 1976. p. 68. [\[CrossRef\]](#)
- [11] Nie X, Leyland A, Song HW, Yerokhin AL, Doney SJ, Matthews A. Thickness effects on the mechanical properties of micro-arc discharge oxide coatings on aluminium alloys. *Surf Coat Technol* 1999;116-119:1055–1060. [\[CrossRef\]](#)
- [12] Aliofkhaezrai M. *Modern surface engineering treatments*. Rijeka: IntechOpen; 2013. p. 10. [\[CrossRef\]](#)
- [13] Ashrafizadeh F. Adhesion evaluation of PVD coatings to aluminium substrate. *Surf Coat Technol* 2000;130:186–194. [\[CrossRef\]](#)
- [14] Dong H. *Surface engineering of light alloys: Aluminium, magnesium and titanium alloys*. UK: CRC Press; 2010. p. 110.
- [15] Rokni MR, Widener CA, Champagne VR. Microstructural stability of ultrafine grained cold sprayed 6061 aluminum alloy. *Appl Surf Sci* 2014;290:482–489. [\[CrossRef\]](#)
- [16] Nie X, Cai R, Zhao C, Sun J, Zhang J, Matthews DTA. Advancement of plasma electrolytic oxidation towards non-valve metals. *Surf Coat Technol* 2022;128403. [\[CrossRef\]](#)
- [17] Kassem M, Fatimah S, Nashrah N, Ko YG. Recent progress in surface modification of metals coated by plasma electrolytic oxidation: Principle, structure, and performance. *Prog Mater Sci* 2021;117:100735. [\[CrossRef\]](#)
- [18] Arslan E, Totik Y, Demirci EE, Vangolu Y, Alsan A, Efeoğlu I. High temperature wear behavior of aluminum oxide layers produced by AC micro arc oxidation. *Surf Coat Technol* 2009;204:829–833. [\[CrossRef\]](#)
- [19] Vangolu Y, Arslan E, Totik Y, Demirci EE, Alsan A. Optimization of the coating parameters for micro-arc oxidation of Cp-Ti. *Surf Coat Technol* 2010;205:1764–1773. [\[CrossRef\]](#)

- [20] Durdu S, Usta M. Characterization and mechanical properties of coatings on magnesium by micro arc oxidation. *Appl Surf Sci* 2012;261:774–782. [\[CrossRef\]](#)
- [21] Kaplan E, Şüküröğlu EE, Çuvalcı O. Investigation of the characterization and tribological behavior of composite oxide coatings doped with h-BN and graphite particles on ZA-27 alloy by micro-arc oxidation. *J Adhes Sci Technol* 2021;35:1305–1319. [\[CrossRef\]](#)
- [22] Kaplan E, Şüküröğlu EE, Çuvalcı O. Investigation of hybrid composite coating on ZA-27 alloy produced by MAO. *SETCI Conference Proceed* 2019;4:379–382.
- [23] Gao C, Xu J, Lan Y, Ma Y, Su W, Liu Y. Preparation of  $\text{Al}_2\text{O}_3/\text{TiO}_2$ -containing coating on aluminium alloys by Micro-arc oxidation. 2010 International Conference on Measuring Technology and Mechatronics Automation; 13-14 March 2010; Changsha, China. [\[CrossRef\]](#)
- [24] Li HX, Song RG, Ji ZG. Effect of nano additive  $\text{TiO}_2$  on performance of micro-arc oxidation coatings formed on 6063 aluminum alloy. *Trans Nonferrous Met Soc China* 2013;23:406–411. [\[CrossRef\]](#)
- [25] Zhang Y, Fan W, Du HQ, Zhao W. Microstructure and wearing properties of PEO coatings: Effect of  $\text{Al}_2\text{O}_3$  and  $\text{TiO}_2$ . *Surf Rev Lett* 2018;25:1850102. [\[CrossRef\]](#)
- [26] Ignjatovic S, Blawert C, Serdechnova M, Karpushenkov S, Damjanovic M, Karlova P, et al. Formation of multi-functional  $\text{TiO}_2$  surfaces on AA2024 alloy using plasma electrolytic oxidation. *Appl Surf Sci* 2021;544:148875. [\[CrossRef\]](#)
- [27] Karaoğlu SY, Karaoğlu S, Unal I. Aerospace industry and aluminum metal matrix composites. *Int J Avi Sci Technol* 2021;02:73-81. [\[CrossRef\]](#)
- [28] Jaspard-Mecuson F, Czerwicz T, Henrion G, Belmonte T, Dujardin L, Viola A, Beauvir J. Tailored aluminium oxide layers by bipolar current adjustment in the plasma electrolytic oxidation (PEO) process. *Surf Coat Technol* 2007;201:8677–8682. [\[CrossRef\]](#)
- [29] Demirbaş C, Ayday A. The influence of nano- $\text{TiO}_2$  and nano- $\text{Al}_2\text{O}_3$  particles in silicate-based electrolytes on microstructure and mechanical properties of micro arc coated Ti6Al4V alloy. *Mat Res* 2018;21:2–6. [\[CrossRef\]](#)
- [30] Mulpur P, Lingam K, Chunduri A, Rattan TM, Rao AM, Kamiseti V. Surface plasmon coupled emission studies on engineered thin film hybrids of nano  $\alpha\text{-Al}_2\text{O}_3$  on Silver. *AIP Conf Proc* 2014;1576:22–24. [\[CrossRef\]](#)
- [31] Mir MA, Shah MA, Ganai PA. Dielectric study of nanoporous alumina fabricated by two-step anodization technique. *Chem Paper* 2021;75:503–513. [\[CrossRef\]](#)
- [32] Chauruka SR, Hassanpour A, Brydson R, Roberts KJ, Ghadiri M, Stitt H. Effect of mill type on the size reduction and phase transformation of gamma alumina. *Chem Eng Sci* 2015;134:774–783. [\[CrossRef\]](#)
- [33] Theivasanthi T, Alagar M. Titanium dioxide ( $\text{TiO}_2$ ) nanoparticles-XRD analyses-An insight. *Chem Phys arXiv:1307.1091*. 2013.
- [34] Scarpelli F, Mastropietro TF, Poerio T, Godbert N. Mesoporous  $\text{TiO}_2$  thin films: State of the art. In: *Titan Dioxide Mater Sustain Environ* 2018:57–80. [\[CrossRef\]](#)
- [35] Li Z, Di S. Microstructure and properties of MAO composite coatings containing nanorutile  $\text{TiO}_2$  particles. *Surf Rev Lett* 2017;24:1750115. [\[CrossRef\]](#)
- [36] Yizhou S, Haijun T, Yuebin L, Xiaofei Z, Tao W, Jie T, Lei P. Fabrication and wear resistance of  $\text{TiO}_2/\text{Al}_2\text{O}_3$  coatings by micro-arc oxidation. *Rare Metal Mat Eng* 2017;46:23–27. [\[CrossRef\]](#)
- [37] Arrabal R, Mohedano M, Matykina E, Pardo A, Mingo B, Merino MC. Characterization and wear behaviour of PEO coatings on 6082-T6 aluminium alloy with incorporated  $\alpha\text{-Al}_2\text{O}_3$  particles. *Surf Coat Technol* 2015;269:64–73. [\[CrossRef\]](#)
- [38] Xue W, Deng Z, Chen R, Zhang T, Ma H. Microstructure and properties of ceramic coatings produced on 2024 aluminum alloy by microarc oxidation. *J Mater Sci* 2001;36:2615–2619.